

Speckle reduction in optical coherence tomography by “path length encoded” angular compounding

N. Iftimia

B. E. Bouma

Harvard Medical School and the Wellman Laboratories
of Photomedicine
Massachusetts General Hospital
50 Blossom Street, BAR 703
Boston, Massachusetts 02114

G. J. Tearney

Harvard Medical School and the Wellman Laboratories
of Photomedicine
Massachusetts General Hospital
Department of Pathology
50 Blossom Street, BAR 703
Boston, Massachusetts 02114
E-mail: tearney@helix.mgh.harvard.edu

Abstract. Speckle, the dominant factor reducing image quality in optical coherence tomography (OCT), limits the ability to identify cellular structures that are essential for diagnosis of a variety of diseases. We describe a new high-speed method for implementing angular compounding by path length encoding (ACPE) for reducing speckle in OCT images. By averaging images obtained at different incident angles, with each image encoded by path length, ACPE maintains high-speed image acquisition and requires minimal modifications to OCT probe optics. ACPE images obtained from tissue phantoms and human skin *in vivo* demonstrate a qualitative improvement over traditional OCT and an increased SNR that correlates well with theory. © 2003 Society of Photo-Optical Instrumentation Engineers. [DOI: 10.1117/1.1559060]

Keywords: speckle reduction; optical coherence tomography; catheters; endoscopes.

Paper 02043 received Jul. 8, 2002; revised manuscript received Oct. 7, 2002; accepted for publication Oct. 7, 2002.

1 Introduction

Optical coherence tomography (OCT) is a promising technique for obtaining high resolution cross sectional images of biological tissues. Clinical OCT studies conducted in the gastrointestinal tract and cardiovascular system have shown that OCT is capable of providing images of the architectural ($>20 \mu\text{m}$) microanatomy of a variety of epithelial tissues, including the layered structure of squamous epithelium and arterial vessels.^{1–3} However, for many important medical applications, such as the early detection of high-grade dysplasia in Barrett’s esophagus and the identification of inflammation within atherosclerotic plaques, visualization of structures that are on a size scale of $<20 \mu\text{m}$ is necessary. State of the art OCT systems, with typical axial resolutions ranging from 8 to 12 μm , have the potential to resolve many of these structures, including nuclei, individual glands, and macrophages. Unfortunately, speckle, which occurs on the same size scale as these features, prohibits unambiguous identification of the cellular and subcellular tissue components required for widespread clinical utilization of this technology.

Catheter or endoscope access and high-speed imaging must be achieved to perform OCT in the internal organs of patients. To minimize diameter, most catheter-based OCT probes employ a single optical fiber to illuminate the sample and detect the signal from the tissue.⁴ High frame rates (typically 4 to 8 frames per second) are required for performing OCT imaging while minimizing artifacts caused by patient motion. A means for reducing speckle in OCT images that does not significantly increase the complexity of single optical fiber probe designs while maintaining high frame rates may be essential for applying OCT to accurately detect and quantify key microscopic tissue structures in patients.

The reduction of speckle in OCT images has been addressed in several recent works. Schmitt described a means for speckle reduction by averaging multiple images acquired at different angles, known as angular compounding.⁵ In this

work, multiple (N) detectors received images acquired from different angles. The images were averaged incoherently, providing an improvement (\sqrt{N}) in the signal to noise ratio (SNR).⁵ While this technique has the advantage that the measurements may be performed in real time, the experimental apparatus as described would not be compatible with a single fiber optic catheter. Bashkansky and Reintjes described an alternative means for angular compounding to reduce speckle.⁶ In this method, translating a retroreflector apparatus in front of the objective lens changed the angle of the incident beam on the tissue. N successive images were acquired and added incoherently to reduce speckle, again improving the SNR by a factor of \sqrt{N} .⁶ While this method is less complex than the use of multiple detectors, the time needed to acquire the images is increased by N . In addition, implementation of this method within the confines of a small diameter catheter or endoscope could be difficult.

We describe a new method for performing angular compounding to reduce speckle within OCT images, angular compounding by path length encoding (ACPE). With ACPE, high-speed acquisition is maintained and modifications to standard OCT catheter optics are minimal.

2 Materials and Methods

A schematic of ACPE is shown in Fig. 1(a). An optical element is inserted prior to the sample arm imaging lens such that portions of the illuminating beam experience different group delays. These new beamlets, now encoded by optical path length, also illuminate the sample at different angles. As a result, multiple OCT images, each acquired at different angles, are present in a single OCT frame [Fig. 1(b)]. When the optical element contains m distinct thicknesses of glass, with each optical thickness a multiple of the others, $2m - 1$ OCT images are obtained in one OCT frame. Each image is

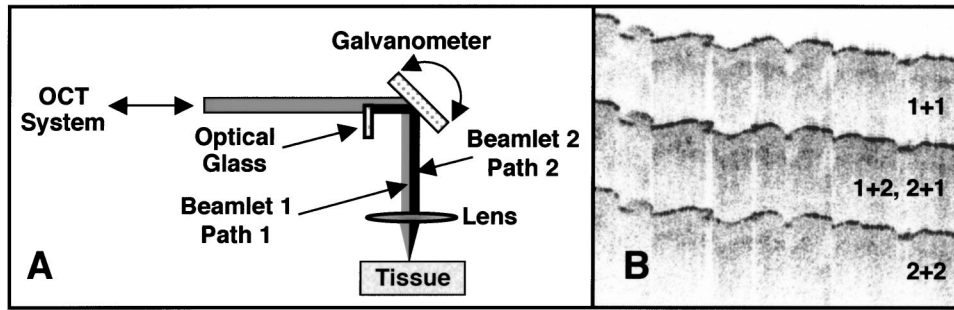


Fig. 1 (a) Schematic of ACPE OCT. An optical glass is placed in the imaging path, splitting the incident field into two beamlets. This optical element causes a portion of the incident beam (beamlet 2) to experience a greater path length delay than beamlet 1. In addition, beamlet 2 illuminates the sample at a different angle than beamlet 1. As a result, multiple OCT images of the specimen, each acquired at a different angle, appear simultaneously on the OCT display (b). In (b), the top image (1+1) corresponds to the image formed from path 1 (incident and reflected), the middle image (1+2,2+1) corresponds to the image formed from path 1 incident, path 2 reflected, and path 2 incident, path 1 reflected. The bottom image (2+2) corresponds to the image formed from path 2 (incident and reflected).

separated by a group delay of $D(n-1)/2$, where D is the thickness and n is the refractive index of the optical material. The distinct OCT images are then averaged to produce a composite OCT image with significantly reduced speckle. Since all of the images are acquired in one OCT frame, single frame acquisition time can be maintained. In addition, the required modifications to the OCT probe involve only the insertion of a small optical element in the beam path of the distal optics. These advantages of ACPE allow speckle averaging to be performed within the confines of a small diameter catheter or endoscope without compromising acquisition speed.

Previous work on OCT speckle reduction by image compounding has shown that the addition of N images of the same intensity provides an SNR increase by a factor of \sqrt{N} .^{5,6} Bashkansky and Reintjes have shown that the speckle distribution in OCT takes the form of the probability density function:

$$p(S_{\text{OCT}}) = \frac{1}{(2\pi\kappa)^{1/2}} \exp\left(-\frac{S_{\text{OCT}}^2}{2\kappa^2}\right), \quad (1)$$

where $\kappa = 2A_R\sigma$, A_R is the amplitude of the reference field, S_{OCT} is the amplitude of the high-pass filtered OCT signal, and σ is its standard deviation.⁶ For this probability density function it can be demonstrated that the SNR improvement obtained by averaging N images of the same amplitude is also a factor of \sqrt{N} , a result that has been experimentally confirmed by Schmitt, and Bashkansky and Reintjes.^{5,6} For ACPE, however, the distinct OCT subimages do not have equal amplitudes, but, assuming isotropic backscattering, they are related to the original OCT image, $S0_{\text{OCT}}$, by β/m^2 , where β is the number of path length combinations that contribute to a distinct subimage. As a result, the SNR for ACPE may be defined as

$$\text{SNR}_{\text{ACPE}} = \frac{\langle S_{\text{OCT}} \rangle}{(\text{var}[S_{\text{OCT}}])^{1/2}} \propto \frac{\sum_{i=1}^N u_i}{(\sum_{i=1}^N u_i^2)^{1/2}}, \quad (2)$$

where u_i is the amplitude of the demodulated OCT signal at a spatial location, and $N = 2m - 1$. In the case of $m = 2$, $N = 3$ images are obtained and the relationships between the amplitudes of the ACPE OCT subimages are $S1_{\text{OCT}} = S3_{\text{OCT}}$

$= 1/4S0_{\text{OCT}}$ and $S2_{\text{OCT}} = 2S1_{\text{OCT}} = 1/2S0_{\text{OCT}}$. The theoretical SNR improvement of the compounded $m = 2$ ACPE image then becomes $\text{SNR}_{\text{ACPE}}/\text{SNR}_0 = 1.63$, where SNR_0 is the signal to noise ratio of $S0_{\text{OCT}}$.

3 Results and Discussion

To test ACPE, we used a polarization-diverse OCT system that has been utilized in previous clinical studies.⁷ OCT images were acquired at 2 frames/s (500 axial pixels \times 500 transverse pixels), displayed with an inverse gray-scale lookup table, and digitally archived. The optical source used in this experiment had a center wavelength of 1310 nm and a bandwidth of 70 nm, providing an axial resolution of approximately 8 μm in tissue.

A modified hand-held galvanometer probe was inserted in the sample arm of the OCT system [Fig. 1(a)]. The objective lens had a focal length of 25 mm and a numerical aperture (NA) of 0.11, providing a measured $1/e^2$ focal spot diameter of 23 μm . A square, antireflection-coated $D = 3.1$ -mm BK7 glass ($n = 1.51$) was inserted between the optical fiber collimator and the objective lens [Fig. 1(a)], so that it overlapped with half of the illuminating beam. With this configuration, we achieved an OCT image separation of approximately 800 μm . When the glass plate was inserted, the spot diameter perpendicular to the glass edge increased by a factor of two (46 μm). In the plane of the OCT image, however, the transverse resolution was preserved.

A solid phantom consisting of 1% Intralipid solution and agar was used to measure the reduction in speckle provided by ACPE. Four hairs were embedded in the Intralipid-agar gel at different transverse positions and depths. A schematic of the phantom is depicted in Fig. 2(a) and the corresponding OCT images without and with the BK7 glass plate are shown in Figs. 2(b) and 2(c), respectively. Insertion of the BK7 glass plate in the sample arm [Fig. 2(c)] produced three copies of the original OCT image [Fig. 2(b)], with each image being acquired at different illumination angles and separated by group delay increments of 800 μm . As predicted, the amplitudes of the signals in the top and bottom images were approximately half that of the center image ($S1_{\text{OCT}}/S2_{\text{OCT}} = S3_{\text{OCT}}/S2_{\text{OCT}} = 1:2$). The ACPE image in Fig. 2(d) was

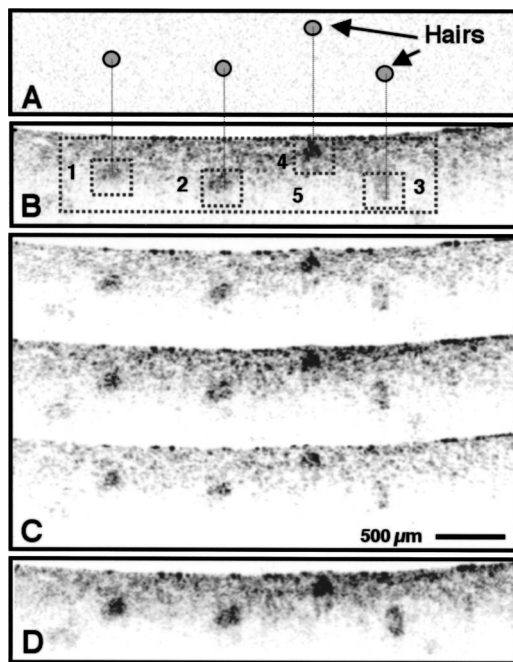


Fig. 2 (a) Schematic of the Intralipid-agar phantom. (b) OCT image of the phantom without insertion of BK7 ACPE element. ROIs labeled 1 to 5 represent locations where the SNR improvement by ACPE was measured. (c) ACPE OCT images obtained by splitting the sample beam in two parts with a 3.1-mm BK7 glass element. (d) Compounded OCT image.

obtained by incoherently averaging the three images in Fig. 2(c). A substantial reduction of speckle in the compounded image can be clearly visualized [Fig. 2(d)]. Compared to the original OCT image, the average ACPE SNR improvement for the five regions depicted in Fig. 2(b) was measured to be 1.54 ± 0.12 (mean \pm standard deviation).

To demonstrate SNR improvement *in vivo*, ACPE OCT imaging was performed on the ventral forearm of a volunteer. Figure 3 shows one representative set of images. Visual assessment of these pictures demonstrates a qualitative improvement in the ACPE image [Fig. 3(b)]. The stratum corneum, epidermis (E) and dermis (D) are more clearly demarcated with ACPE [Fig. 3(b)]. In addition, horizontal structures consistent with dermal vasculature are more easily

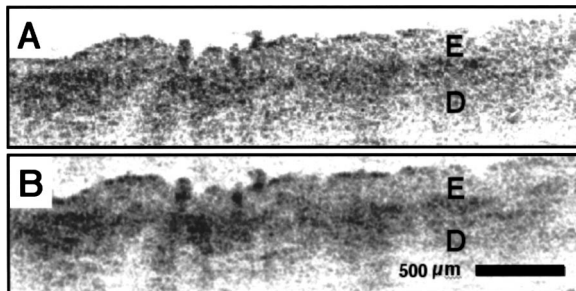


Fig. 3 (a) OCT image of the ventral forearm obtained *in vivo* prior to insertion of the BK7 ACPE element. (b) Compounded ACPE OCT image of the skin acquired at the same location as that in (a).

identified in the ACPE image [Fig. 3(b)]. The SNR was measured for the ACPE and original OCT images in Fig. 3, yielding an SNR improvement of 1.56.

In this work, we have demonstrated a novel method for reducing speckle in OCT images that does not decrease the OCT frame rate and requires only minor modifications to the OCT probe. The implementation of ACPE, however, requires compromises between speckle reduction and three other important OCT system parameters: 1. sample arm transverse resolution, 2. total reference arm path length, and 3. OCT image sensitivity. First, for any given objective lens, ACPE compromises the transverse resolution in one dimension by underfilling the lens aperture for each individual beamlet. In most cases, increasing the numerical aperture (NA) of the objective can compensate for this resolution loss.

Speckle averaged ACPE OCT images can be obtained at the same rate as conventional OCT images by scanning an increased reference arm path length delay at the same frequency. To acquire each of the individual OCT subimages, the new scan length of the ACPE OCT system needs to be $L(2m - 1)$, where L is the original scan length of the OCT system. Using phase control RSOD lines,⁸ scan ranges up to 10 mm are possible, enabling $m = 3$, $L = 2$ mm, and a maximum predicted SNR improvement of ~ 2.1 .

Increasing the reference arm path length scan range while maintaining the scan rate, however, increases the electronic bandwidth and decreases the sensitivity of the OCT system. Also, because ACPE splits the sample arm power into $2m - 1$ subimages, each subimage contains a fraction of the original sample arm power. When imaging human tissue, these losses primarily affect the penetration depth of the OCT image. Since many features of clinical relevance, such as nuclei in patients with Barrett's esophagus or macrophages in atherosclerotic plaques, are present at tissue surfaces, we expect that for modest m , the improvements in image quality provided by ACPE will outweigh sensitivity losses. Moreover, ongoing technical developments toward more efficient interferometer designs^{9,10} and higher power, clinically viable OCT sources may render ACPE sensitivity losses a nonissue.^{11,12}

The thickness of the path length encoding optical element described (3.1 mm BK7) may not be sufficient for OCT imaging in some tissues, as it only provided 800- μ m separation between individual subimages. Increasing the thickness of the BK7 glass to 7.7 mm would allow a path length separation of 2 mm. This thickness would be adequate for free-space, handheld OCT probes, but would be problematic in small diameter, flexible catheters, where minimizing the rigid length is of importance. To increase the optical thickness of the path length encoding element, a higher refractive index material such as silicon ($n = 3.5$) may be used. To create a 2-mm delay with silicon, only 1.6 mm of the material would be needed. When using high-refractive index glass, however, dispersion imbalances between the reference and sample arms must be considered. For high-resolution OCT imaging ($\Delta\lambda/\lambda > 10\%$), appropriate selection of the optical material used for path length encoding will depend on the center wavelength and bandwidth of the source.

To conclude, we have demonstrated a novel method for reducing speckle in OCT images that does not increase the OCT frame rate and requires the addition of only a single passive element in the OCT probe. These features of ACPE

make it compatible with OCT imaging in internal organ systems in patients. While implementation of ACPE necessitates tradeoffs between speckle reduction and system sensitivity, the problems caused by speckle noise are arguably more significant for clinical diagnosis than the penetration depth of modern OCT systems, especially at 1300 nm. Since difficulties in interpreting features on the size scale of 20 μm or less is in part a result of speckle noise in OCT images, we expect that ACPE will greatly improve the capabilities of OCT for the diagnosis of important diseases such as dysplasia and inflammation in atherosclerosis.

Acknowledgments

This research is supported in part by the Center for Integration of Medicine and Innovative Technologies (CIMIT) and the Whitaker Foundation.

References

1. B. E. Bouma, G. J. Tearney, C. C. Compton, and N. S. Nishioka, "High-resolution imaging of the human esophagus and stomach in vivo using optical coherence tomography," *Gastrointest. Endosc.* **51**, 467–474 (2000).
2. A. Das, M. Sivak, A. Chak, R. Wong, V. Westphal, A. Rollins, J. Willis, G. Isenberg, and J. Izatt, "High-resolution endoscopic imaging of the GI tract: a comparative study of optical coherence tomography versus high-frequency catheter probe EUS," *Gastrointest. Endosc.* **54**, 219–224 (2001).
3. I. K. Jang, B. E. Bouma, D. H. Kang, S. J. Park, S. W. Park, K. B. Seung, K. B. Choi, M. Shishkov, K. Schlendorf, E. Pomerantsev, S. L. Houser, H. T. Aretz, and G. J. Tearney, "Visualization of coronary atherosclerotic plaques in patients using optical coherence tomography: comparison with intravascular ultrasound," *J. Am. Coll. Cardiol.* **39**, 604–609 (2002).
4. G. J. Tearney, S. A. Bopart, B. E. Bouma, M. E. Brezinski, N. J. Weissman, J. F. Southern, and J. G. Fujimoto, "Scanning single-mode fiber optic catheter-endoscope for optical coherence tomography," *Opt. Lett.* **21**, 543–545 (1996).
5. J. M. Schmitt, "Array detection for speckle reduction in optical coherence microscopy," *Phys. Med. Biol.* **42**, 1427–1429 (1997).
6. M. Bashkansky and J. Reintjes, "Statistics and reduction of speckle in optical coherence tomography," *Opt. Lett.* **25**, 545–547 (2000).
7. B. E. Bouma and G. J. Tearney, "Power-efficient nonreciprocal interferometer and linear-scanning fiber optic catheter for optical coherence tomography," *Opt. Lett.* **24**, 531–533 (1999).
8. G. J. Tearney, B. E. Bouma, and J. G. Fujimoto, "High-speed phase and group-delay scanning with a grating-based phase control delay line," *Opt. Lett.* **22**, 1811–1813 (1997).
9. A. M. Rollins and J. A. Izatt, "Optical interferometer designs for optical coherence tomography," *Opt. Lett.* **24**, 1484–1486 (1999).
10. B. E. Bouma and G. J. Tearney, "Power-efficient nonreciprocal interferometer and linear-scanning fiber-optic catheter for optical coherence tomography," *Opt. Lett.* **24**, 531–533 (1999).
11. B. E. Bouma, G. J. Tearney, I. P. Bilinsky, B. Golubovic, and J. G. Fujimoto, "Self-phase modulated Kerr lens mode-locked Cr: fosterite laser source for optical coherence tomography," *Opt. Lett.* **21**, 1839–1841 (1996).
12. C. Chudoba, J. G. Fujimoto, E. P. Ippen, H. A. Haus, U. Morgner, F. X. Kartner, V. Scheuer, G. Angelow, and T. Tschudi, "All-solid-state Cr: fosterite laser generating 14-fs pulses at 1.3 μm ," *Opt. Lett.* **26**, 292–294 (2001).